Available online at www.sciencedirect.com
ScienceDirect
Building and Environment 43 (2008) 1046–1054
BUILDING AND ENVIRONMENT
www.elsevier.com/locate/buildenv

Experimental energy and exergy analysis of a double-flow solar air heater having different obstacles on absorber plates

Hikmet Esen*

Department of Mechanical Education, Faculty of Technical Education, Fırat University, 23119 Elazığ, Turkey

Received 27 June 2006; received in revised form 22 January 2007; accepted 23 February 2007

Abstract

This paper presents an experimental energy and exergy analysis for a novel flat plate solar air heater (SAH) with several obstacles and without obstacles. For increasing the available heat-transfer area may be achieved if air is flowing simultaneously and separately over and under the different obstacle absorbing plates, instead of only flowing either over or under the different obstacle absorbing plates, leading to improved collector efficiency. The measured parameters were the inlet and outlet temperatures, the absorbing plate temperatures, the ambient temperature, and the solar radiation. Further, the measurements were performed at different values of mass flow rate of air and different levels of absorbing plates in flow channel duct. After the analysis of the results, the optimal value of efficiency is middle level of absorbing plate in flow channel duct for all operating conditions and the double-flow collector supplied with obstacles appears significantly better than that without obstacles. At the end of this study, the exergy relations are delivered for different SAHs. The results show that the largest irreversibility is occurring at the flat plate (without obstacles) collector in which collector efficiency is smallest.

Keywords: Solar air heater; Experimental; Exergy analysis; Double-flow; Obstacles; Thermal efficiency

1. Introduction

The main applications of solar air heaters (SAHs) are space heating and drying. The SAHs occupy an important place among solar heating systems because of minimal use materials. Low heat transfer coefficients result from the unfavourable thermophysical properties of air, which are widely used in different thermal systems. The efficiency of SAH has been found to be low because of low convective heat transfer coefficient between absorber plate and the flowing air which increases the absorber plate temperature, leading to higher heat losses to the environment resulting in low thermal efficiency of such collectors. The remedy is to improve the heat transfer, which can be achieved by creating a fully turbulent flow in these systems. There are different factors affecting the SAH efficiency, e.g. collector length, collector depth, type of absorber plate, glass cover plate, wind speed, etc. The absorber plate shape factor is the most important parameter in the design for any type of SAH. Increasing the absorber plate shape area will increase the heat transfer to the flowing air, but on the other hand, will increase the pressure drop in the collector; this increases the required power consumption to pump the air flow crossing the collector [1].

Several configurations of SAHs have been developed in literature. Various designs, with different shapes and dimensions of the air flow passage in plate type solar air collectors were tested [2–7]. The double-flow type SAHs have been introduced for increasing the heat-transfer area, leading to improved thermal performance [5]. This increases the thermal energy between the absorber plate and the air, which clearly improves the thermal performances of the solar collectors with obstacles arranged into the air channel duct. These obstacles allow a good distribution of the fluid flow [8,9].

In history, there has been a noticeable increase of interest in the applications of second law analysis to the design of thermal systems [10]. A typical thermal design based on the first law of thermodynamics allows us to address issues

*Tel.: +90 424 237 0000/4228; fax: +90 424 236 7064.
E-mail address: hikmetesen@firat.edu.tr.

0360-1323/$ - see front matter © 2007 Elsevier Ltd. All rights reserved.
doi:10.1016/j.buildenv.2007.02.016

Nomenclature

A_C	surface area of the collector (m^2)
C_P	specific heat of air at constant pressure (kJ/kg K)
$\dot{E}$	energy rate (kW)
$\dot{E}x$	exergy rate (kW)
$\dot{E}x_{dest}$	rate of irreversibility (kW)
I	solar radiation (W/m^2)
$\dot{m}$	mass flow rate (kg/s)
M	mass (kg)
t	time (s, min)
T	temperature (°C)
U	heat loss coefficient ($W/m^2\,°C$)
$\dot{W}$	work rate or power (kW)
$w_{\dot{m}}$	total uncertainty of mass flow rate (%)
w_η	total uncertainty of efficiency (%)
w_F	total uncertainty of $(T_{in}-T_a)/\dot{E}x_{dest}$ (%)

Greek letters

η	thermal efficiency (dimensionless)
η_{II}	exergetic efficiency (dimensionless)
η_0	optical yield (dimensionless)
Ψ	specific exergy (kJ/kg)

Subscripts

a	air
ave	average
C	collector
c	convection
e	environment
f	fluid
in	inlet
out	outlet
p	plate
r	radiation
s	surface

related to the energy balance of the system. The second law of thermodynamic analysis combined with a standard design procedure of a thermal system gives us invaluable insight into the operation of the system. However, exergy analysis, derived from both the first and second laws of thermodynamics, as compared to energy analysis, takes into account the quality of the energy transferred. The main purpose of the exergy analysis is to determine the reasons of the thermodynamic faults of the thermal and chemical processes. Exergy (or availability) analysis is a powerful tool in the design, optimization, and performance evaluation of energy systems. This analysis can be used to identify the main sources of irreversibility (exergy loss) and to minimize the generation of entropy in a given process where the transfer of energy and material take place [11,12]. According to Dincer and Rosen [13], exergy analysis is an effective thermodynamic scheme for using the conservation of mass and energy principles together with the second law of thermodynamics for the design and analysis of thermal systems, and is an efficient technique for revealing whether or not and by how much it is possible to design more efficient thermal systems by reducing the inefficiencies. The concepts and definitions of exergy analysis are well recognized [14–17].

The studies on exergy analysis of SAHs are relatively few [18–20]. Öztürk and Demirel [18] presented an experimental investigation of the thermal performance of a SAH having its flow channel packed with Raschig rings. They observed that the energy and exergy efficiencies of the packed-bed SAH increased as the outlet temperature of heat transfer fluid increased. Öztürk [19] described an experimental evaluation of energy and exergy efficiency of a seasonal latent heat storage system for greenhouse heating with the SAH. Ucar and Inalli [20] presented thermal and exergy analysis of SAHs with passive augmentation techniques.

In this paper, we present a comparison between the results obtained in the case of the double-flow solar air collector supplied with obstacles and those of the collector without obstacles. An experimental set-up, described in the next section, is constructed and tested in Technical Education Faculty of Fırat University, Elazığ, Turkey. The efficiency of the SAH is determined from the experimental measurements. The influences of various parameters, such as the obstacles of absorber plate, the mass flow rate of air and the level of absorber plates in duct on the energetic and exergetic efficiencies of the SAH are examined, and the significant variables are identified.

2. Description of the experimental set-up and measurement procedure

Turkey also has great solar energy potential due to its location in the Mediterranean Region (36° and 42° North latitudes). The sunshine period of Turkey is 2624 h/year with a maximum of 365 h/month in July and a minimum of 103 h/month in December. The main solar radiation intensity is about 3.67 kWh/m^2 day. The cumulative total of this is about 1.340 MWh/m^2 year. The amount of solar radiation received over all of Turkey, in other words, the gross solar energy potential is 3517 EJ/year [19].

A schematic view of the constructed double-flow SAH system and front view sight of collector are shown in Fig. 1(a) and (b), respectively, and photographs of the four different absorber plates of the SAH collector are shown in Figs. 2(a)–(d), respectively. Fig. 3 gives the variations of meteorological data (mean monthly ambient temperatures, °C, and mean monthly solar radiation, cal/cm^2min)

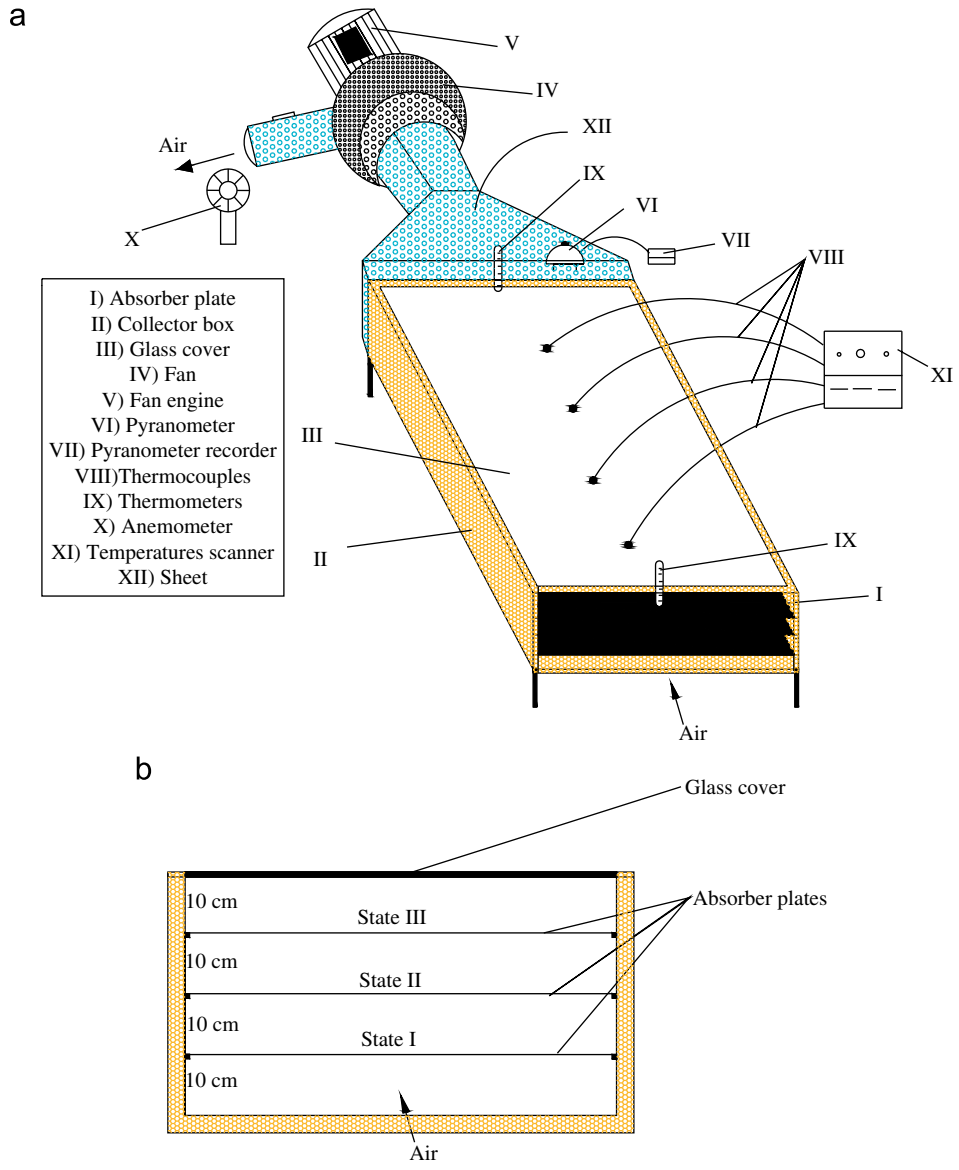

Fig. 1. Schematic assembly of the (a) SAH system and (b) front view of collector.

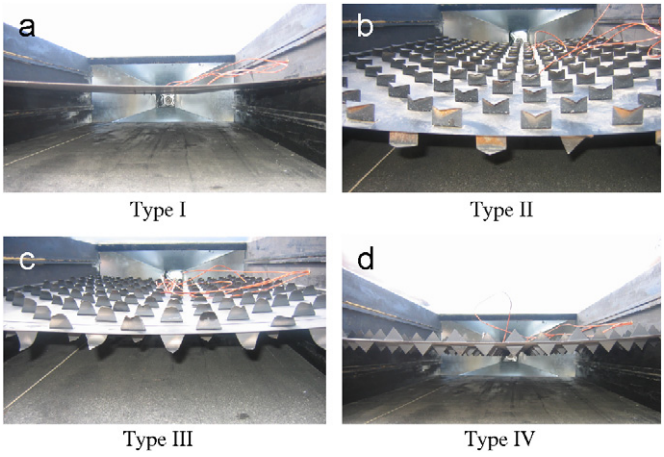

Fig. 2. Types of absorber plates.

measured in Elazığ (latitude 38.41°N, longitude 39.14°E, altitude 1067 m above sea level) by the Elazığ State Meteorological Station from 1995 to 2005. Fig. 4 also shows variation of the mean monthly ambient temperature and mean monthly solar radiation in 2005 [21].

In this study, four types of absorber plates were used. The absorbers were made of stainless steel with black chrome selective coating. Dimension and plate thickness for all four collectors were 1.25 m, 0.8 m, and 1 mm, respectively. Normal window glass of 5 mm thickness was used as glazing. Single cover glass was used in all four collectors. Thermal losses through the backs of the collector are mainly due to the conduction across the insulation (thickness 3 cm) and those caused by the wind and the thermal radiation of the insulation are assumed negligible.

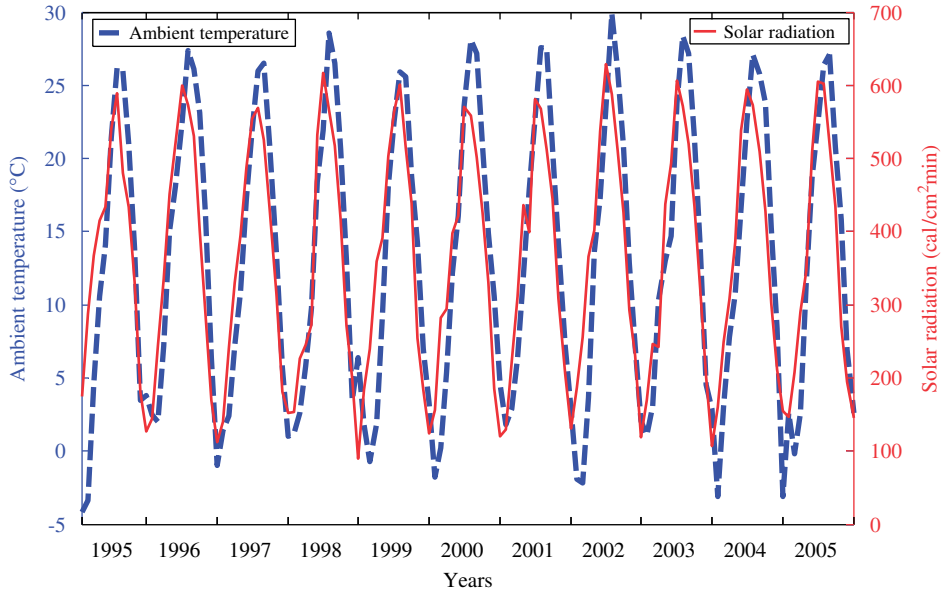

Fig. 3. Meteorological yearly data for the 1995–2005 period in Elazığ [21].

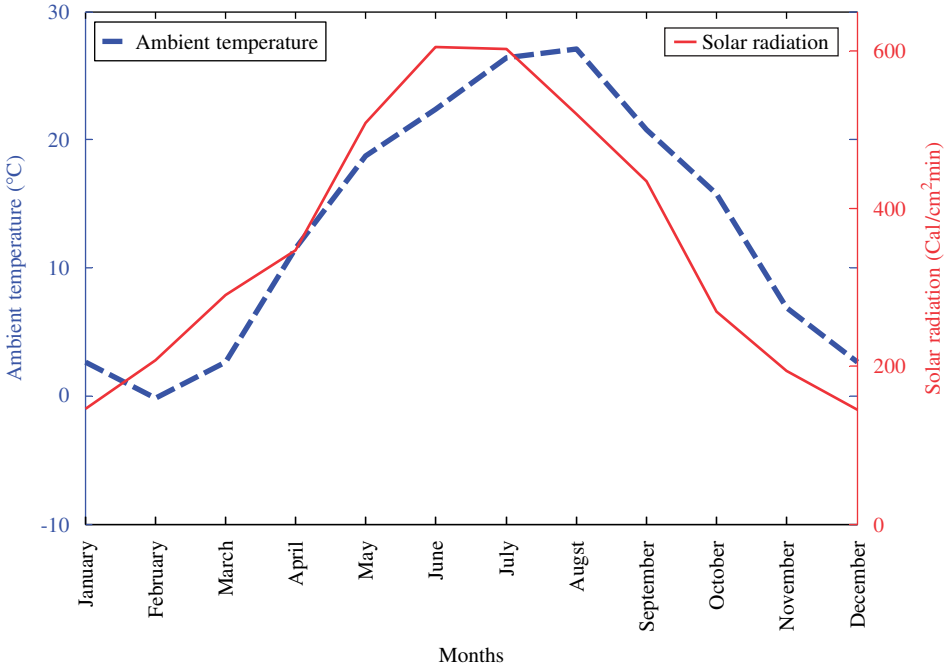

Fig. 4. Meteorological monthly data for 2005 in Elazığ [21].

After installation, the four collectors were left operating several days under normal weather conditions for weathering processes. Thermocouples were positioned evenly, on the top surface of the absorber plates, at identical positions along the direction of flow, for four collectors. Inlet and outlet air temperatures were measured by two well-insulated thermocouples. The ambient temperature was measured by a mercury thermometer placed in a special container behind the collectors body. The total solar radiation incident on the surface of the collector was measured with a Kipp and Zonen CM 11 Pyranometer. This meter was placed adjacent to the glazing cover, at the same plane, facing due south. The total solar radiation was recorded by a Kipp and Zonen CC 12 solar integrator automatically. The measured variables were recorded at time intervals of 30 min and include: insolation, inlet and outlet temperatures of the working fluid circulating through the collectors, ambient temperature, absorber plate temperatures at several selected locations, and air flow rates (Lutron AM-4206 M digital anemometer). The air was provided by a radial fan with a maximum of 0.537 kW power. The radial fan placed at the outlet of the

collectors sucked in the air. The pressure loss was measured by means of a digital manometer (AZ 82100) placed between inlet and outlet of the collector. All tests began at 9 am and ended at 4 pm.

3. Thermal analysis and uncertainty

The theoretical model employed for the study of the solar collector that operates in unsteady state is made using a thermal energy balance [22]:

$$[\text{Accumulated energy}] + [\text{Energy gain}] = [\text{Absorbed energy}] - [\text{Lost energy}]; \quad (1)$$

for each term of Eq. (1) the following expressions are formulated:

$$[\text{Accumulated energy}] = M_p C_p (dT_{p,ave}/dt), \quad (2)$$

$$[\text{Energy gain}] = \dot{m} C_p (T_{out} - T_{in}), \quad (3)$$

$$[\text{Absorbed energy}] = \eta_o I A_C, \quad (4)$$

$$[\text{Lost energy}] = U_C (T_{p,ave} - T_e) A_C. \quad (5)$$

By combining Eqs. (2)–(5), the thermal energy balance equation necessary to describe the solar collector functioning is obtained:

$$M_p C_p (dT_{p,ave}/dt) + \dot{m} C_p (T_{out} - T_{in}) = \eta_o I A_C - U_C (T_{p,ave} - T_e) A_C. \quad (6)$$

The optical yield (η_o) and the energy lose coefficient (U_C) are the parameters that characterize the behaviour of the solar collector. Note that η_o represents the fraction of the solar radiation absorbed by the plate and depends mainly on transmittance of the transparent covers and on the absorbance of the plate [22].

The energy loss coefficient includes the losses by the upper cover, the laterals, and the bottom of the collector. The upper cover losses prevail over the others, depending to a large extent on the temperature and emissivity of the absorbent bed, and besides, on the convective effect of the wind on the upper cover.

The thermal efficiency of the solar collectors (η) is defined as the ratio between the energy gain and the solar radiation incident on the collector plane:

$$\eta = \dot{m} C_p (T_{out} - T_{in})/(I A_C). \quad (7)$$

Uncertainty analysis (the analysis of uncertainties in experimental measurement and results) is a powerful tool, particularly when it is used in the planning and design of experiments.

The result R is a given function in terms of the independent variables. Let w_R be the uncertainty in the result and $w_1, w_2, \ldots, w_n$ be the uncertainties in the independent variables. The result R is a given function of the independent variables $x_1, x_2, x_3, \ldots, x_n$. If the uncertainties in the independent variables are all given with same odds, then uncertainty in the result having these odds is calculated by [23]

$$w_R = \left[\left(\frac{\partial R}{\partial x_1} w_1 \right)^2 + \left(\frac{\partial R}{\partial x_2} w_2 \right)^2 + \cdots + \left(\frac{\partial R}{\partial x_n} w_n \right)^2 \right]^{1/2}. \quad (8)$$

The independent parameters measured in the experiments reported here are: collector inlet temperature, collector outlet temperature, ambient temperature, air velocity and pressure in the duct, and solar radiation. To carry out these experiments, T-type thermocouples with an accuracy of 0.018 °C, a metal vane type anemometer (AM-4206 M, air velocity + air flow) with ±2% accuracy, pressure transducer with ±0.3% (at ±25 °C) accuracy (AZ 82100, digital manometer) and Kipp and Zonen CM 11 Pyranometer with 1% accuracy were used.

From these measured data, collector efficiency, mass flow rate and $(T_{in}-T_a)/I$ were calculated [24]. Equation for efficiency is

$$\eta = \dot{m} C_p (T_{out} - T_{in})/(I A_C).$$

If A_C and C_p are considered constants, it can be written:

$$\eta = f(T_{out}, T_{in}, I, \dot{m}); \quad (9)$$

equation for mass flow rate is

$$\dot{m} = \rho A_c v. \quad (10)$$

As density of air ρ is dependent on pressure P and temperature T, the following relationship can be estimated:

$$\dot{m} = f(v, T, P). \quad (11)$$

Following Eq. (8), total uncertainty for mass flow rate can be written as

$$w_{\dot{m}} = \left[\left(\frac{\partial \dot{m}}{\partial v_{air}} w_{v_{air}} \right)^2 + \left(\frac{\partial \dot{m}}{\partial T_{air}} w_{T_{air}} \right)^2 + \left(\frac{\partial \dot{m}}{\partial P_{air}} w_{P_{air}} \right)^2 \right]^{1/2}. \quad (12)$$

Similarly, the total uncertainty for collector efficiency and $(T_{in}-T_a)/I$ can be written as

$$w_\eta = \left[\left(\frac{\partial \eta}{\partial \dot{m}} w_{\dot{m}} \right)^2 + \left(\frac{\partial \eta}{\partial T_{out}} w_{T_{out}} \right)^2 + \left(\frac{\partial \eta}{\partial T_{in}} w_{T_{in}} \right)^2 + \left(\frac{\partial \eta}{\partial I} w_I \right)^2 \right]^{1/2}, \quad (13)$$

$$w_F = \left[\left(\frac{\partial F}{\partial T_{in}} w_{T_{in}} \right)^2 + \left(\frac{\partial F}{\partial T_{out}} w_{T_{out}} \right)^2 + \left(\frac{\partial F}{\partial I} w_I \right)^2 \right]^{1/2}, \quad (14)$$

where

$$F = \frac{T_{in} - T_a}{I}.$$

The total uncertainty in determining flow rate, efficiency, and $(T_{in}-T_a)/I$ were estimated by Eqs. (12)–(14), respectively. Calculations show that the total uncertainty in

calculating mass flow rate of air, efficiency and $(T_{in}-T_a)/I$ are 45.62%, 1.82% and 1%, respectively.

4. Exergy analysis of case study

This article focuses on the combination of the two laws of thermodynamics, which are described in the concept of exergy analysis.

The assumptions made in the analysis presented in this study are:

(i) steady state, steady flow operation,
(ii) negligible potential and kinetic energy effects and no chemical or nuclear reactions,
(iii) air is an ideal gas with a constant specific heat, and its humidity content is ignored,
(iv) the directions of heat transfer to the system and work transfer from the system are positive.

The mass balance equation can be expressed in the rate form as

$$\sum \dot{m}_{in} = \sum \dot{m}_{out}, \tag{15}$$

where $\dot{m}$ is the mass flow rate, and the subscript in stands for inlet and out for outlet.

If the effects due to the kinetic and potential energy changes are neglected, the general energy and exergy balances can be expressed in rate form as given below [20]:

$$\sum \dot{E}_{in} = \sum \dot{E}_{out}, \tag{16}$$

$$\sum \dot{E}x_{in} - \sum \dot{E}x_{out} = \sum \dot{E}x_{dest}, \tag{17a}$$

or

$$\dot{E}x_{heat} - \dot{E}x_{work} + \dot{E}x_{mass,in} - \dot{E}x_{mass,out} = \dot{E}x_{dest}. \tag{17b}$$

Using Eq. (17b), the rate form of the general exergy balance can also be written as

$$\sum \left(1-\frac{T_e}{T_s}\right)\dot{Q}_s - \dot{W} + \sum \dot{m}_{in}\psi_{in} - \sum \dot{m}_{out}\psi_{out} = \dot{E}x_{dest}, \tag{18}$$

where

$$\psi_{in} = (h_{in} - h_e) - T_e(s_{in} - s_e), \tag{19}$$

$$\psi_{out} = (h_{out} - h_e) - T_e(s_{out} - s_e). \tag{20}$$

If Eqs. (19) and (20) are substituted in Eq. (18), it is arranged that

$$\left(1-\frac{T_e}{T_s}\right)\dot{Q}_s - \dot{m}[(h_{out} - h_{in}) - T_e(s_{out} - s_{in})] = \dot{E}x_{dest}, \tag{21}$$

where $\dot{Q}_s$ is solar energy absorbed by the collector absorber surface and it is evaluated by the expression [25]:

$$\dot{Q}_s = H(\tau\alpha)A_c. \tag{22}$$

The enthalpy and entropy changes of the air in the collector are expressed by [20]

$$\Delta h = h_{out} - h_{in} = c_p(T_{f,out} - T_{f,in}), \tag{23}$$

$$\Delta s = s_{out} - s_{in} = c_p \ln\frac{T_{f,out}}{T_{f,in}} - R\ln\frac{P_{out}}{P_{in}}. \tag{24}$$

Substituting Eqs. (22)–(24) in Eq. (21), it may be rewritten as

$$\left(1-\frac{T_e}{T_s}\right)H(\tau\alpha)A_c - mc_p(T_{f,out} - T_{f,in}) + mc_pT_e\ln\frac{T_{f,out}}{T_{f,in}} - mRT_e\ln\frac{P_{out}}{P_{in}} = \dot{E}x_{dest}. \tag{25}$$

The irreversibility $\dot{E}x_{dest}$ can be directly evaluated from the following equation:

$$\dot{E}x_{dest} = T_eS_{gen}. \tag{26}$$

The second law efficiency is calculated as

$$\eta_{II} = 1 - \frac{T_eS_{gen}}{[1-(T_e/T_s)]\dot{Q}_s}. \tag{27}$$

All physical properties of air were selected according to the following bulk mean temperature:

$$\Delta T_m = (T_{in} + T_{out})/2. \tag{28}$$

5. Results and discussions

Collector performance tests were conducted on days with clear sky condition. The collector slope was adjusted to 38°, which is considered suitable for the geographical location of Elazığ. The collectors were instrumented with T-type thermocouples for measuring temperatures of flowing air at inlet and outlet of the collector, and the ambient temperature.

The collector efficiency improvements for double-pass type SAHs were calculated using Eq. (7). Various air mass flow rates between 0.015 and 0.025 kg/s are also investigated at the experiments. Experimental studies had been performed during the one month (01.07.2005–31.07.2005) period.

Fig. 5 shows the hourly variation of efficiencies of Types (I–IV) at State-II and mass flow rate is 0.02 kg/s, respectively, during the a month period. The mean efficiencies for Type I, Type II, Type III, and Type IV are found to be 38%, 43%, 45%, and 41%, respectively. The hourly measured solar radiation is also shown in Fig. 5. As expected, it increases in the morning to a peak value of 926 W/m^2 at noon and starts to decrease in the afternoon. As shown the efficiencies increase to a maximum value at 12:30 pm in the noon, before it starts to decrease later in the afternoon. As seen from the figure, the efficiency of Type-III (great turbulence) is higher than that of Type-II (middle turbulence), than that of Type IV (little turbulence) and also that of Type I (no turbulence, without obstacles), respectively. The study has shown that

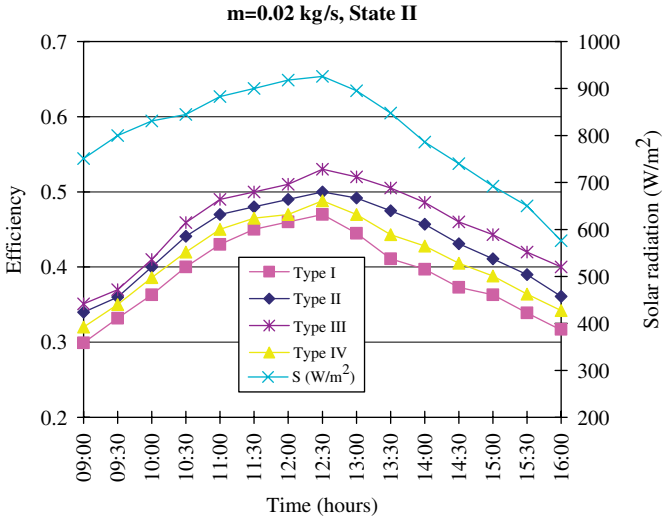

Fig. 5. Variation of collector efficiency at different types of absorber plates.

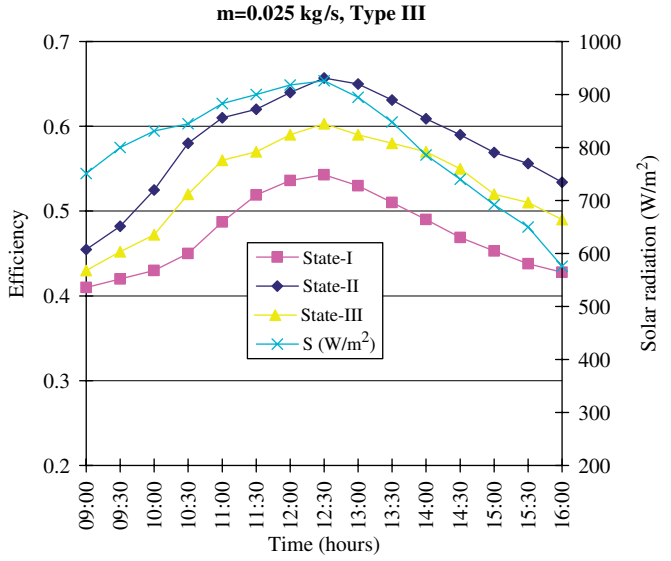

Fig. 6. Variation of collector efficiency at different state collectors.

the solar collector supplied with Type III than Type I leads to a very significant improvement in the efficiency–temperature rise couple. It's because Type III leads to very great turbulence in the collector unit.

Fig. 6 depicts the hourly variation of the efficiency of Type III collector at different states (I–II–III, see Fig. 1b). The mean efficiencies for State-I, State-II and State-III are found to be 46%, 58%, and 53%, respectively. It is seen from Fig. 6 that the optimal value of efficiency is middle level of the collector for all operating conditions. This means that in order to achieve the best efficiency in a double-flow SAH, in which the cross-section areas of upper and lower flow channels are constructed equally, the mass flow rates in both flow channels must be the same. The efficiency decreases when lower channel, as well as upper channel, goes away from mid-point collector. The obtained results in this study are very similar to those shown in Ref. [5]. According to this reference, double-flow type SAHs had been introduced for increasing the heat-transfer area, leading to improved efficiency. From the results obtained for the different solar collector types examined, we deduce that the introduction of the obstacles in the air channels is a very important factor for the improvement of collector efficiency. However, we have observed that the form, dimensions, orientation, and disposition of the obstacles considerably influence the collector efficiency.

Fig. 7 illustrates the hourly variation of the efficiency of Type III collector at State-II, for different mass flow rates (0.015, 0.02, 0.025 kg/s). The results show that the collector

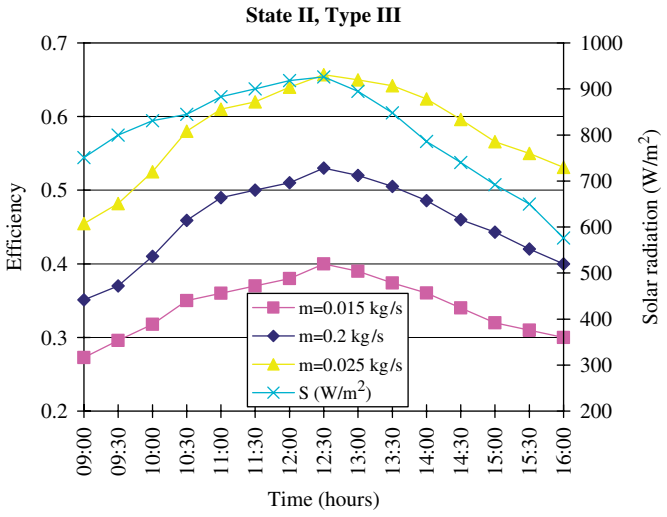

Fig. 7. Variation of collector efficiency at different mass flow rates.

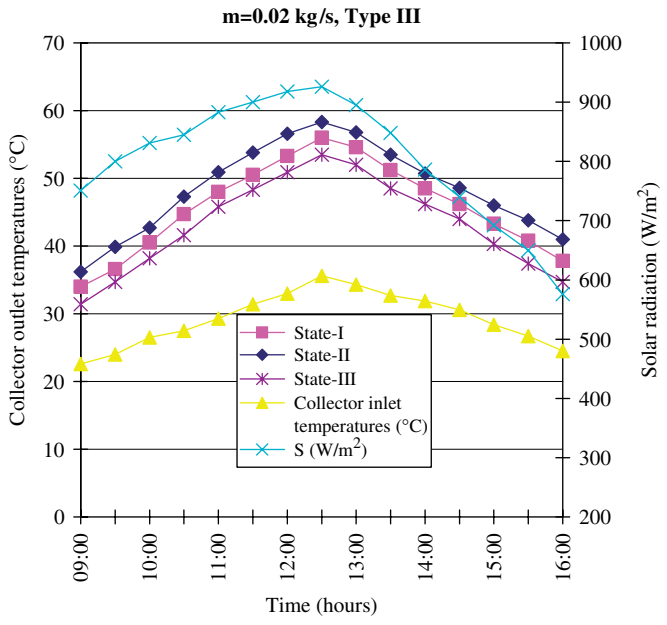

Fig. 8. Variation of inlet and outlet collector temperatures at different states.

Table 1
Exergy analysis of tested SAHs

Solar col.	Mass flow rate (kg/s)	Exergy input, $\dot{E}x_{in}$(kW)			Exergy output, $\dot{E}x_{out}$ (kW)			Irreversibility, $\dot{E}x_{dest}$ (kW)			Exergy loss (%)			Second law efficiency, η_{II} (%)		
		State I	State II	State III	State I	State II	State III	State I	State II	State III	State I	State II	State III	State I	State II	State III
Type I	0.015	0.39	0.381	0.385	0.10	0.111	0.105	0.29	0.27	0.28	74.35	70.86	72.72	25.65	29.14	27.28
	0.2	0.381	0.372	0.375	0.10	0.120	0.11	0.281	0.252	0.265	73.75	67.74	70.66	26.25	32.26	29.34
	0.025	0.375	0.340	0.355	0.11	0.115	0.112	0.265	0.225	0.243	70.66	66.17	68.45	29.34	33.83	31.55
Type II	0.015	0.351	0.342	0.347	0.138	0.140	0.139	0.213	0.202	0.208	60.68	59.06	59.94	39.32	40.94	40.06
	0.2	0.341	0.330	0.335	0.143	0.148	0.145	0.198	0.182	0.19	58.06	55.15	56.71	41.94	44.85	43,29
	0.025	0.33	0.324	0.327	0.148	0.155	0.15	0.182	0.169	0.177	55.15	52.16	54.12	44.84	47.84	45.88
Type III	0.015	0.31	0.328	0.316	0.145	0.170	0.155	0.165	0.158	0.161	53.22	48.17	50.94	46.78	51.83	49.06
	0.2	0.32	0.321	0.318	0.150	0.180	0.175	0.17	0.141	0.143	53.12	43.92	44.96	46.88	56.08	55.04
	0.025	0.30	0.310	0.314	0.148	0.189	0.180	0.152	0.121	0.134	50.66	39.03	42.67	49.34	60.97	57.33
Type IV	0.015	0.362	0.351	0.355	0.118	0.12	0.119	0.244	0.231	0.236	67.4	65.81	66.47	32.6	34.19	33.53
	0.2	0.350	0.34	0.35	0.121	0.125	0.123	0.229	0.215	0.227	65.42	63.23	64.87	34.58	36.77	35.13
	0.025	0.343	0.331	0.338	0.131	0.129	0.13	0.212	0.202	0.208	61.8	61.02	61.53	38.2	38.98	38.47

efficiency increases with increasing air mass flow rate of air $\dot{m}$ and solar radiation I.

Fig. 8 shows that the hourly variation of the inlet and outlet collector temperatures of Type III at mass flow rate is 0.02 kg/s, for all states. The results show that the collector inlet and outlet temperatures increase with the solar radiation I. As shown, the inlet air temperature increases to a maximum value of 35.6 °C at 12:30 pm before it starts to decrease in the afternoon. The outlet air temperature increases to a peak value of 58.9 °C at 13:00 pm and then decreases as solar radiation drops to lower values later during the day.

Irreversibility of each of SAH has been calculated and the results have been shown in Table 1. The exergy analysis was carried out in July of 2005 in Elazığ for different mass flow rates, different types of collectors, and different states of absorber plates. It can be seen that Type I is the collector in which the exergy loss is the highest (74.35%, for 0.015 kg/s and State I). In Type III with each staggered absorber plate, exergy loss is the lowest (39.03%, for 0.025 kg/s and State II). Furthermore, the second law efficiency or exergetic efficiency of each of SAHs has been calculated. It is clear from Table 1 that the point of the lowest η_{II} typically occurs in Type I (25.65%, for 0.015 kg/s and State I). The maximum η_{II} occurs in Type III (60.97%, for 0.025 kg/s and State II).

6. Conclusions

A detailed experimental study was conducted to evaluate the energetic and exergetic efficiencies of four types of double-flow solar air collectors under a wide range of operating conditions. According to the results of the experiments, the double-flow type of the SAHs has been introduced for increasing the heat-transfer area, leading to improved thermal and exergetic efficiencies. The optimal value of efficiency is middle level (State-II) of collector for all operating conditions. In addition, this study has allowed us to show that the use of obstacles in the air flow duct of the double-flow collector is an efficient method of adapting in air exchanger according to user needs. Test results always yield higher efficiency values for Type III than for Type I (without obstacles) flat plate collector. The obstacles ensure a good air flow over and under the absorber plates, create the turbulence, and reduce the dead zones in the collector.

The largest irreversibility occurs at the flat plate SAH (Type I), since, in flat plate collector (Type I) only a little part of solar energy absorbed by the collector can be used in the exergy analysis.

Consequently, given the different operative and atmospheric conditions that can happen in practice, it must be taken into account the possibility of scheming different experiences, in order to determine the influence of the different variables on the collector efficiency and the characteristic parameters of the solar collector.

References

[1] Kabeel AE, Mecarik K. Shape optimization for absorber plates of solar air collectors. Renewable Energy 1998;13(1):121–31.
[2] Hollands KGT, Shewan EC. Optimization of flow passage geometry for air-heating, plate-type solar collectors. Transactions of ASME, Journal of Solar Energy Engineering 1981;103:323–30.
[3] Choudhury C, Garg HP. Design analysis of corrugated and flat plate solar air heaters. Renewable Energy 1991;1(5/6):595–607.
[4] Hachemi A. Thermal performance enhancement of solar air heaters, by fan-blown absorber plate with rectangular fins. International Journal of Energy Research 1995;19(7):567–78.
[5] Yeh HM, Ho CD, Hou JZ. The improvement of collector efficiency in solar air heaters by simultaneously air flow over and under the absorbing plate. Energy 1999;24(10):857–71.

[6] Hegazy AA. Performance of flat plate solar air heaters with optimum channel geometry for constant/variable flow operation. Energy Conversion and Management 2000;41(4):401–17.
[7] Yeh HM, Ho CD, Lin CY. Effect of collector aspect ratio on the collector efficiency of upward type baffled solar air heaters. Energy Conversion and Management 2000;41(9):971–81.
[8] Zaid AA, Messaoudi H, Abenne A, Ray ML, Desmons JY, Abed B. Experimental study of thermal performance improvement of a solar air flat plate collector through the use of obstacles: application for the drying of "yellow onion". International Journal of Energy Research 1999;23(12):1083–99.
[9] Moummi N, Ali SY, Moummi A, Desmons JY. Energy analysis of a solar air collector with rows of fins. Renewable Energy 2004;29(13):2053–64.
[10] Bejan A. Research needs in thermal systems. New York: ASME; 1986 (Chapter Second law analysis: the method for maximising thermodynamic efficiency in thermal systems).
[11] Bejan A. In: Advanced engineering thermodynamics. New York: Wiley Interscience; 1988. p. 501–14.
[12] Kotas TJ. In: The exergy method of thermal plant analysis. London: Butterworths; 1994. p. 197.
[13] Dincer I, Rosen MA. Exergy as a driver for achieving sustainability. International Journal of Green Energy 2004;1(1):1–19.
[14] Kotas TJ. The exergy method of thermal plant analysis. Malabar, FL: Krieger; 1995 (reprint ed.).
[15] Bejan A. Entropy generation minimization. Boca, Raton, FL: CRC Press; 1996.
[16] Bejan A, Tsatsaronis G, Moran M. Thermal design and optimization. New York: Wiley; 1996.
[17] Wark K. Advanced thermodynamics for engineers. New York: McGraw-Hill; 1995.
[18] Öztürk HH, Demirel Y. Exergy-based performance analysis of packed-bed solar air heaters. International Journal of Energy Research 2004;28(5):423–32.
[19] Öztürk HH. Experimental evaluation of energy and exergy efficiency of a seasonal latent heat storage system for greenhouse heating. Energy Conversion and Management 2005;46(9–10):1523–42.
[20] Ucar A, Inalli M. Thermal and exergy analysis of solar air collectors with passive augmentation techniques. International Communications in Heat and Mass Transfer 2006;33(10):1281–90.
[21] Elazığ State Meteorological Station. Records for weather and solar radiation data's in Elazığ, Turkey, 2005.
[22] Albizzati E. Inclusión de Temas Relacionados con la Energía Solar en Cursos de las Carreras de Ingeniería. In: Proceeding of the millennium solar forum 2000: International Solar Energy Society. México DF, September 17–22; 2000. pp. 663–66 (in Spanish).
[23] Holman JP. Experimental methods for engineers, 6th ed. Singapore: McGraw-Hill; 1994.
[24] Karim MA, Hawlader MNA. Performance investigation of flat plate, v-corrugated and finned air collectors. Energy 2006;31(4):452–70.
[25] Torres-Reyes E, Navarrete-Gonzalez JJ, Zaleta-Aguilar Z, Cervantes-de Gortari JG. Optimal process of solar to thermal energy conversion and design of irreversible flat-plate solar collectors. Energy 2003;28(2):99–113.